Ballistic magnetoresistance in nickel single-atom conductors without magnetostriction

Matthew R. Sullivan, Douglas A. Boehm, Daniel A. Ateya, Susan Z. Hua, and Harsh Deep Chopra*
Thin Films and Nanosynthesis Laboratory, Materials Program, Mechanical and Aerospace Engineering Department, State University of New York at Buffalo, Buffalo, New York 14260, USA
(Received 15 April 2004; revised manuscript received 26 July 2004; published 18 January 2005)

Large ballistic magnetoresistance (BMR) has been measured in Ni single-atom conductors electrodeposited between microfabricated thin films. These measurements eliminate magnetostriction related artifacts. By making measurements on single atom conductors, the *benchmark* for the incontrovertible evidence against magnetostriction is set at the unyielding condition of the known quantum mechanical principles, namely, $1G_o = 2e^2/h = 1/12\,900\Omega^{-1}$ (for ferromagnetic contacts the unit of conductance being $\frac{1}{2}G_o = 1/25\,800\Omega^{-1}$) is the universal threshold ballistic conductance of an *unbroken* single atom contact below which even an angstrom separation of the contact due to magnetostriction is immediately signaled by an abrupt and large increase in tunneling resistance of several hundred thousand ohms across the gap. The present approach to electrodeposited point contacts between microfabricated thin films also provides an independent confirmation of Garcia's original BMR experiments on atomic point contacts that were made by a mechanical method [N. Garcia, M. Muñoz, and Y.-W. Zhao, Phys. Rev. Lett. **82**, 2923 (1999)]. There are many intricacies and subtleties to be resolved and understood in the highly interesting BMR phenomenon. Conclusive elimination of magnetostriction related artifacts, which is most easily invoked as a primary alternative explanation to the electronic origin of BMR, is one step towards a better understanding of these atomic scale entities. In addition, several explanations of null effects in some of the reported literature are given.

DOI: 10.1103/PhysRevB.71.024412 PACS number(s): 75.47.Jn, 73.23.Ad, 72.25.Ba

Spin dependent electron transport across a single atom represents the ultimate miniaturization of spintronics devices. Garcia, Muñoz, and Zhao[1] reported several hundred percent ballistic magnetoresistance (BMR) in atomic point contacts of Ni made by a mechanical method, and subsequently observed 400–700 % BMR in electrodeposited Ni nanocontacts made between bulk Ni lead wires.[2,3] Large magnetoresistance effect has also been reported in half-metal magnetite (Fe_3O_4) point contacts made by a mechanical method.[4,5] Using experiments similar to Garcia's, we have recently reported several thousand percent BMR effect in electrodeposited Ni nanocontacts formed between bulk Ni wires.[6,7] Similar BMR values have since been reported.[8] While much progress has been made in recent years towards understanding the origin of the BMR effect, it is also accompanied by uncertainty and controversy that invariably follows the maturation of any new field or discovery. Various possible interpretations and their validity under different circumstances are discussed in detail later in the paper; possible reasons for null results in some of the reported articles are also discussed.

For BMR, difficulty lies in separating the electronic origin of the effect from signals that could possibly be attributed to magnetostriction and other artifacts. In this regard, study of nanocontacts deposited between substrate-constrained thin films is an important first step in removing these uncertainties because sample can be made reproducibly. However, it is not sufficient in itself. Experiments must be designed in which the contraction or elongation of the nanocontact due to magnetostriction, and other artifacts would immediately and unambiguously manifest itself.

Fortunately, for magnetostriction such an unambiguous experiment can be designed by exploiting the quantized nature of conductance in ballistic conductors made of a single atom.[9] In metals where the Fermi wavelength of the electrons is typically of the order of 0.5 nm, the transverse confinement of the electron wave functions by the narrow contact diameter quantizes the energy levels (channels), with each channel contributing to the total conductance in discrete units of $2e^2/h(\equiv G_o)$; e is the charge of the electron and h is the Planck's constant.[10–12] In the case of a ferromagnetic contact, the spin degeneracy can be lifted, causing the stepwise change in conductance to occur in units of $\frac{1}{2}G_o$ instead of G_o;[13,14] spin-splitting and magnetoconductance has even been reported in (oxidized) Cu point contacts.[15,16] The separation between the channels increases with a decrease in the contact diameter, causing an increasing number of channels to rise above the Fermi level and become unavailable for conductance. In the limit of a single atom contact, only a single channel is left below the Fermi level, for a total conductance of $1G_o(=2e^2/h=1/12\,900\Omega^{-1})$—the resistance associated with a contact so narrow that there is only a single (transverse) mode of current transmission, see Refs. 17–19. In other words, the conductance plateau of $1G_o = 1/12\,900\Omega^{-1}$ (or $\frac{1}{2}G_o = 1/25\,800\Omega^{-1}$ in a spin-split ferromagnetic contact) is a *universal* and *discrete threshold* for an unbroken atomic point contact. As soon as the contact is broken, the ballistic transport with its transversally quantized wave functions is replaced by tunneling where the wave functions are now longitudinally confined across the narrow gap. This transition is signaled by an abrupt and large exponential increase in resistance from the universal ballistic threshold of 12 900Ω (or 25 800Ω) to tunneling resistance of several hundred thousand ohms. *This is an unyielding condition of the known quantum mechanical principles, and it unambiguously determines whether the atomic point contact is*

broken or intact. Nickel has negative magnetostriction and it contracts in the direction of an applied magnetic field. Therefore even an angstrom separation of the single atom Ni contact from adjacent Ni leads due to magnetostriction will immediately signal a broken contact. *Hence magnetoconductance measurements on single atom Ni contacts offer an unambiguous experiment in ascertaining the absence or presence of magnetostriction related artifacts in BMR*.

Single atom Ni contacts were electrodeposited between microfabricated thin-film leads of Ni on silicon wafers. High resistance <100> silicon wafers coated with an additional 1 μm thick silicon dioxide insulator layer were used to suppress any possible leakage currents through the substrate during subsequent electrodeposition and testing. Special microfabrication steps were taken to keep the starting gap between the patterned thin film leads to be as small as possible (1 μm) in order to ensure that the leads are maximally constrained by the substrate. This was achieved by using photolithography to first form 0.4–0.5 μm deep channels on the silicon wafer by reactive ion etching, as shown in the scanning electron microscope (SEM) image in Fig. 1(a). A Ta (3 nm)/Ni (10 nm) seed layer was sputter deposited inside the channels on which Ni was subsequently electrodeposited. The channel was 50 μm wide. The final thickness of electrodeposited Ni was ~2 μm, and having approximately the same width as the channel. Electrodeposition of Ni on the seed layer reduces the gap to <0.5 μm due to lateral growth of the electrodes once the thickness exceeds the channel depth, Fig. 1(b). Since the 0.4–0.5 μm high channel walls initially restrict the lateral growth of the films, sufficiently thick Ni films with low lead resistance (3–5Ω) could thus be electrodeposited. This serves as the starting point for making the nanocontacts between the two electrodes and contact formation across the submicron gap does not change these overall electrode dimensions. The final contact is made by using the lead with the microfabricated tip as cathode and the opposite lead as anode. The patterned tip on the cathode facilitates the formation of the atomic contacts across it. The micrograph in Fig. 1(b) also highlights the preservation of the patterned tip geometry during electrodeposition to thicken the seed layer. In addition to the film being adherent to the substrate and by the side walls of the channels, the films were further constrained on the top by epoxy. Epoxy served a twofold purpose. First, the insulation serves to reduce leakage currents during electrodeposition (in the pA range of less). Second, epoxy additionally constrains the films even from the top.

Nickel was electrodeposited at room temperature using nickel sulfamate solution [84 g/l Ni as metal in $Ni(SO_3NH_2)_2.2H_2O$; 30 g/l boric acid, pH 3.3] at a deposition voltage between −0.7 and −1.0 V versus a saturated calomel electrode. The single atom conductors were made using the self-terminating method of Tao.[20] In particular this simple and elegant method allows electrodeposition of stable nanocontacts to a size-resolution of a single atom. Following the formation of the contact the electrical measurements were made at a voltage ranging from 200 mV to 350 mV. While the atomic sized samples are stable for over 1 minute, they cannot withstand the oxidation in air for long periods of time and mechanical shocks during the solution exchange

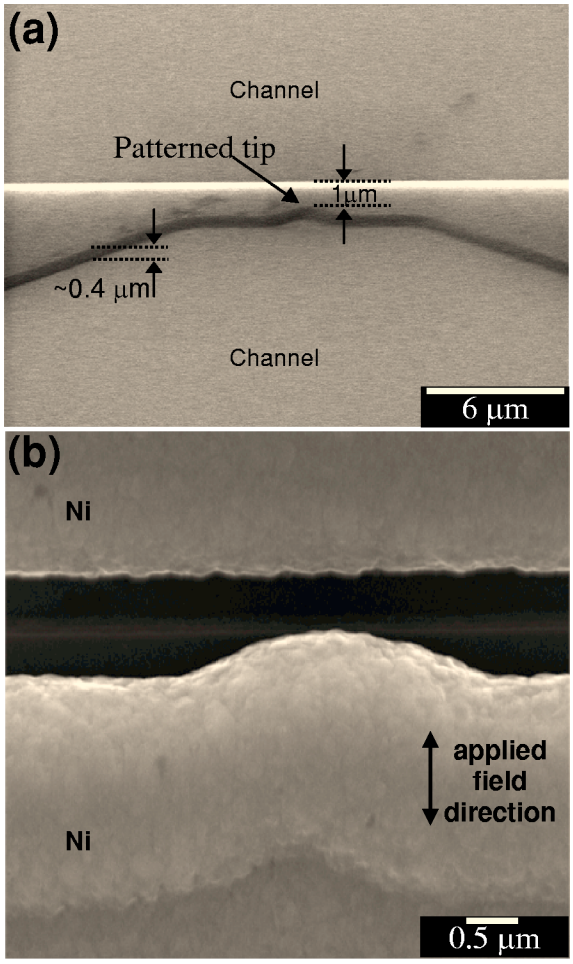

FIG. 1. (a) SEM micrograph showing 0.4–0.5 μm deep microfabricated channels on oxidized silicon wafer in which Ni thin film leads were subsequently electrodeposited. Note the 1 μm initial gap between the channels. (b) SEM micrograph showing thin film leads made by electrodeposition of Ni on a previously sputter deposited Ta/Ni seed layer inside the channels. The final contact between thin film leads is made by electrodeposition of Ni until the lead with the tip joins the opposite lead.

(and add uncertainty to the measurements). However this is not a problem. It is well known that the theoretical potential for electrodeposition of Ni is over 400 mV,[21] and experimentally one requires greater than 0.7–0.8 V for deposition due to over-potential. Additionally we have experimentally confirmed absence of any change in contact size (or chemistry) by measuring the I/V curves for different sized atomic contacts. The I/V curves in Fig. 2 show linear behavior in the measured voltage range showing no change in contact size (or chemistry). More recently we have also succeeded in measuring I/V curves in deionized distilled water (to prevent air oxidation) and found them to be identical to those measured in the solution.

Figure 3(a) shows an example of a stable single atom Ni conductor at a conductance plateau of $1G_o$ made by the self-terminating method. Figure 3(b) shows another example of a stable single atom Ni conductor that was grown to the targeted conductance plateau of $1G_o$. In Fig. 3(b) the conduc-

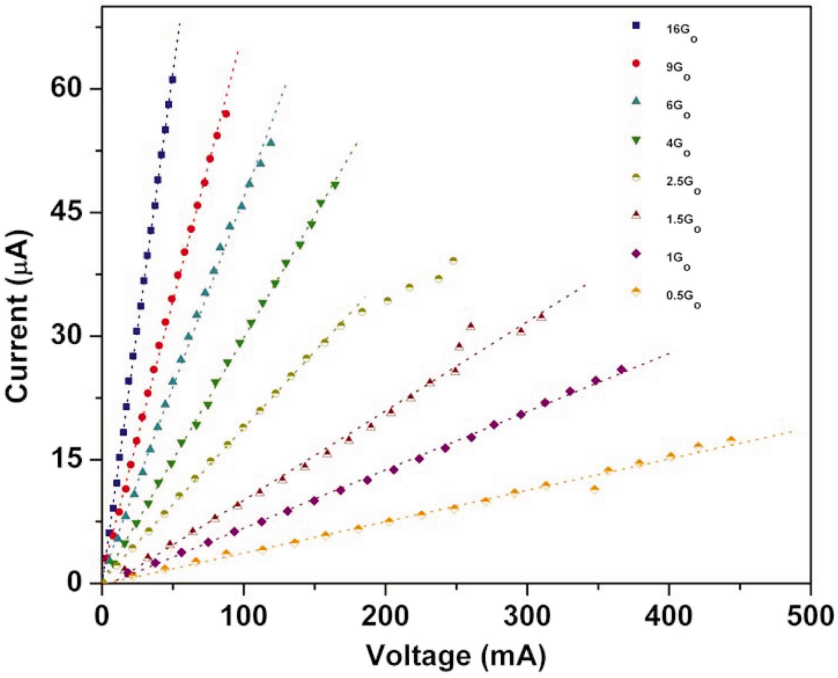

FIG. 2. (Color) *I-V* curves of Ni contacts at different conductance plateaus. The dotted line is a linear fit of the data. Similar curves are obtained when measured in contacts immersed in deionized, ultrafiltered water.

tance curve during the growth of the contact rises to the stable $1G_o$ plateau in a stepwise fashion with the brief appearance of the $\frac{1}{2}G_o$ plateau even though no magnetic field was present during the electrodeposition. Previously, half-integral multiples of G_o have been observed in Ni nanocontacts formed (by mechanical methods) in the presence of an applied magnetic field, and attributed to a field-induced single domain state in the Ni wires adjacent to the contact.[13,14] In our study it was found that even in the absence of an applied magnetic field the conductance often stabilized spontaneously at half-integral multiples of G_o.[22] Therefore the spontaneous appearance of such spin-split states in contacts made in zero field is indicative of a single domain state in the vicinity of the contact, and is not entirely unexpected given the overall small dimensions of the contact and the thin film leads in the vicinity of the contact (however there are micromagnetic subtleties that arise once the contacts are swept in the field, as later described in the discussion of the micromagnetic structure). Figure 3(c) shows a conductance plot for a single atom contact that has spontaneously stabilized in a spin-split state of $\frac{1}{2}G_o$. As shown in Fig. 3(c), initially when a gap is present between the leads, the resistance is very high (0.5–1.0 MΩ). As soon as the contact is formed, the conductance makes an abrupt jump and spontaneously stabilizes at the $\frac{1}{2}G_o$ conductance plateau. Figure 3(d) shows another example of a single atom contact that has stabilized in its $\frac{1}{2}G_o$ spin-split state.

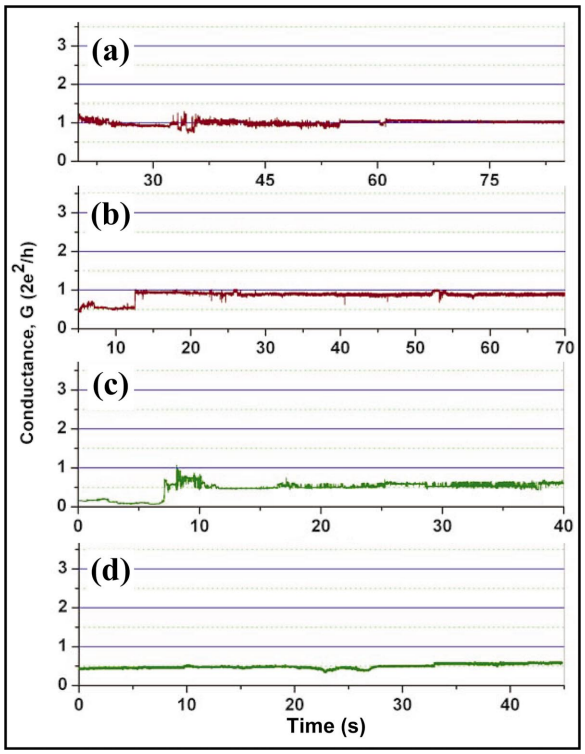

FIG. 3. (Color) Conductance plots for four different single atom conductors stabilized at (a) and (b) $1G_o$, and (c) and (d) $\frac{1}{2}G_o$ conductance plateaus.

Figures 4(a) and 4(b) show, respectively, the magnetoconductance of single atom Ni conductors stabilized at $\frac{1}{2}G_o$ and $1G_o$ conductance plateaus. In addition, Figs. 4(c) and 4(d) show the magnetoconductance of samples that were stabilized at $\frac{3}{2}G_o$, and $2G_o$ plateaus, respectively. The corresponding curves for resistance versus field are also shown in Figs. 4(a)–4(d). Each sample in Fig. 4 was stabilized at its respective conductance plateau for a sufficiently long period of time prior to applying the magnetic field. The direction of the continuous applied field is along the axis of the contact joining the thin film leads, as shown in Fig. 1(b); the magnetic field was manually swept and the shown dependence of R versus H while approximate does not alter the nature of the results. As shown in Fig. 4(a), the conductance of the single atom conductor changes from a stable value of $\frac{1}{2}G_o(\sim 25.8\ \text{k}\Omega)$ in zero field to $5G_o(\sim 2.6\ \text{k}\Omega)$ at 500 Oe.

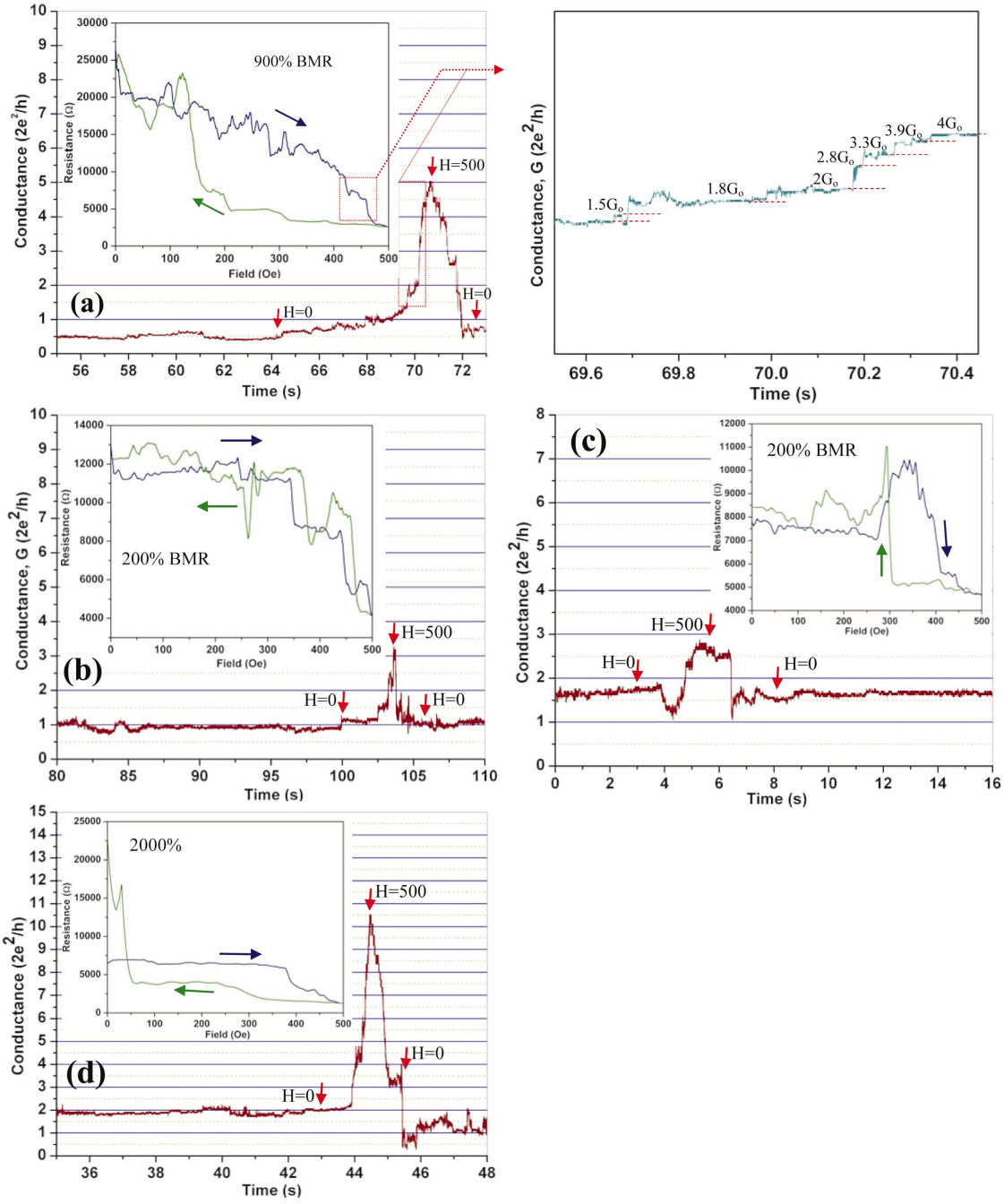

FIG. 4. (Color) Magnetoconductance and magnetoresistance of single atom Ni conductors stabilized at (a) $\frac{1}{2}G_o$, (b) $1G_o$, (c) $\frac{3}{2}G_o$, and (d) $2G_o$. The inset in (a) shows the nonquantized but discrete jumps as the sample is being cycled in applied field. The magnetic field was manually swept and the shown dependence of R versus H while approximate does not alter the nature of the results. The MR curves are for one quadrant of applied field only. Conversion from conductance to resistance values amplifies data (including noise) by a factor of ~13 000, and the resistance data is averaged over adjacent point to avoid this.

Once the field is removed the conductance drops back to its zero-field plateau. Since the sample has low conductance (or high resistance) at zero field and a high conductance (lower resistance) at high field, this represents a negative BMR effect of ~900%. The inset in Fig. 4(a) is discussed later. Figure 4(b) shows another single atom conductor that was stabilized at $1G_o$ prior to applying the magnetic field. As in Fig. 4(a) the sample in Fig. 4(b) also shows an increase in conductance with increasing field, rising from $1G_o$(~13 kΩ) at zero field to $3G_o$(4.3 kΩ) at 500 Oe, and dropping back reversibly to $1G_o$ once the field is turned off, giving a 200% BMR effect. The samples stabilized at $\frac{3}{2}G_o$, and $2G_o$ plateaus in Figs. 4(c) and 4(d), respectively, similarly show a negative BMR effect of 200% and 2000%, respectively. Note that the conductance plateaus of $\frac{3}{2}G_o$, and $2G_o$ also likely represent the magnetoconductance behavior of single Ni atom conductors albeit in different electronic channels, see Refs. 17–19, since the open d shell of Ni is

capable of carrying multiple channels/atom (even without considering the effect of *s* and *p* orbitals, which can potentially lead to an even greater number of channels per Ni atom). Also, Fig. 4(c) is shown deliberately to underscore the value of making magnetoconductance measurements at $\frac{1}{2}G_o$ and $1G_o$ as in Figs. 4(a) and 4(b), since the dip in conductance in Fig. 4(c) preceding the eventual increase in conductance would otherwise be harder to interpret due to magnetostriction related artifacts. A closer examination of these MR curves show that the conductance does not change continuously as a function of applied magnetic field, but it does not necessarily take only quantized values (in units of $1G_o$ or $\frac{1}{2}G_o$). This is highlighted in the inset of Fig. 4(a), which is taken from the circled portion of the conductance trace in Fig. 4(a). While it is well known from extensive past literature and the present study that the growth of contacts occurs by the system taking only quantized values, manifestation of a fine structure points to something far more intricate as to how the energy landscape is being altered during the application of magnetic field. We do not yet have extensive systematic data, and studies to this effect are currently underway to further explore this very interesting behavior.

Nickel has negative magnetostriction (saturation magnetostriction strain $\lambda_s = -34 \times 10^{-6}$).[23,24] Therefore a first step in minimizing the role of magnetostriction is to prevent the sample from freely changing its physical dimensions. In the present study, the microfabricated thin film leads are constrained by the substrate and by the microfabricated channels in which the leads are partially embedded. This constraint is further maximized by minimizing the starting gap between the leads, which is 1 μm as shown in Fig. 1(a). Only in this short segment the leads have no seed layer underneath. The maximum contraction strain for every μm of free length l is given by $\Delta l = \lambda_s l$, giving a maximum possible elongation of -0.034 nm, or ~ -0.3 Å, which is only a fraction of the atomic diameter of Ni.[24] Even the presence of this minuscule elongation cannot be ruled out *a priori*, and hence the necessity of using single atom conductors in making an unambiguous interpretation. Any residual magnetostriction contraction in the leads due to this micron long segment would tend to break the contact and lower the conductance. Since the measurements were made on single atom conductors, this would be signaled by a large and instantaneous drop in conductance of the order of several hundred thousand ohms even for an angstrom separation. *Contrary to this*, the magnetoconductance of single atom conductors in Figs. 4 *increases* rather than decreases in response to an applied magnetic field, conclusively ruling out the role of magnetostriction in these measurements. The results also show an impressive mechanical robustness of these seemingly fragile entities. Considering that in terms of size these single atom Ni conductors are most delicate compared to their larger counterparts, they also represent the litmus test for the susceptibility of larger contacts to break apart due to magnetostriction. It is also important to note that the first reported BMR measurements by Garcia were done on atomic point contacts of Ni between bulk Ni wires using a mechanical method.[1] The present study uses an entirely different experimental technique to reproduce Garcia's results, an important yardstick to resolve any scientific controversy.

In recent years extensive work has been done in building a theoretical framework for explaining the origin of the BMR effect.[25–31] Within a contact, the presence of a magnetic dead layer enhancing spin polarization and producing large BMR values has been proposed.[25] Other models invoke the existence of atomically sharp constrained domain walls as being responsible for enhanced spin scattering. The concept of mechanically constrained domain walls residing inside a nanocontact itself was first put forward by Bruno.[32] Such constrained domain walls can be atomically sharp (compared to hundreds of nanometers wide conventional domain walls), and their behavior has been simulated and theoretically studied by several groups in recent years, e.g., Savchenko *et al.*,[33] Molyneux *et al.*,[34] Coey *et al.*[35] Imammura and Kobayashi have shown that large magnetoresistance effect can occur in the presence of such atomically sharp domain walls and magnetoresistance oscillates with the width of the contact.[26] The oscillatory behavior remains to be characterized with progress in making stable point contacts. Tagirov and co-workers have done extensive and in-depth theoretical work on the BMR effect and found that the MR is a multivalued function of the quantized conductance.[27–30] Their observations help explain the fluctuations in the observed magnitude of the BMR effect and shows an enormous enhancement in MR at a few open channels and provides a quantum mechanical framework for the realization of a quantum spin valve. Another important contribution to the theoretical understanding of the BMR effect is due to the recent work by Velev and Butler.[31] Their work specifically deals with magnetoresistance enhancements for certain contact geometries having narrow necks and aspect ratios, such as the ones in the present study. These studies provide an accumulating theoretical framework for understanding the contacts in the present study.

Next consider the micromagnetic structure and various subtleties that invariably are entailed and remain to be resolved in the investigation of these atomic scale entities. While the constrained domain walls have yet to be imaged due to resolution limitations of instrumentation and short life spans of the contacts, we have investigated the micromagnetic structure as a function of electrode geometry, film composition, and film thickness to understand how an antiparallel aligned state may best be realized across the leads in zero field. Our results to date show a single domain Ni state across the electrodes in zero field *provided* the electrodes are *thin* (10-20 nm). In such cases we find no BMR effect and also because the contacts are difficult to form. In contrast, we find clear evidence of a multidomain structure across the electrodes in sufficiently thick Ni electrodes, as in the present study; even thicker films with larger gain size would be preferred but involves greater fabrication challenges. As a reference point for this discussion, Figs. 5(a)–5(d) show several zero-field micromagnetic micrographs in electrodes made of 50 nm thick permalloy film (prior to forming a contact). These micrographs clearly show antiparallel magnetic domains in the opposite electrodes in zero field. These images were taken by using the interference contrast colloid or ICC method, which is discussed in detail elsewhere.[36] The direction of magnetization in these micrographs was determined by applying a small magnetic field, which helps reveal

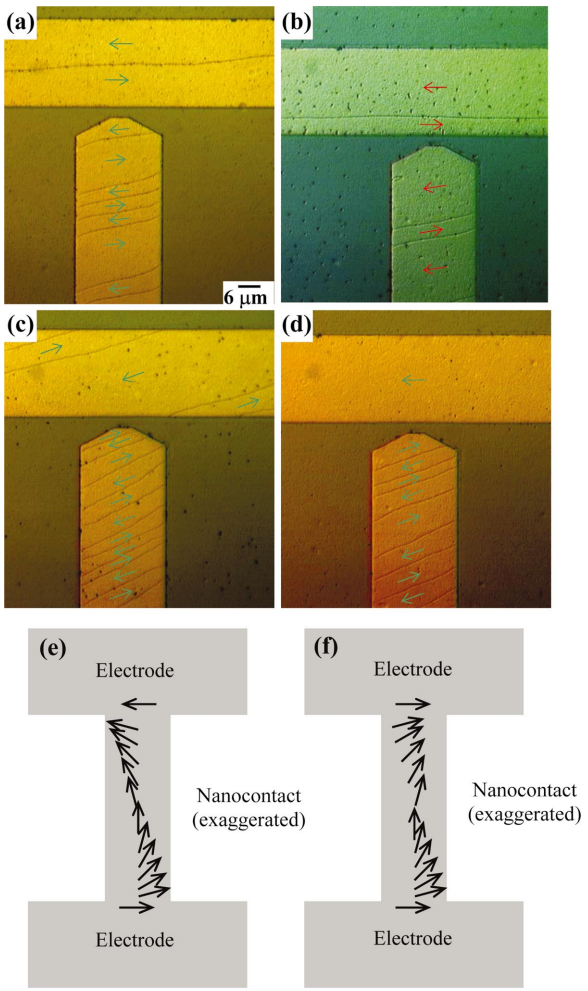

FIG. 5. (Color) (a)–(d) Micromagnetic structures in electrodes made of 50 nm permalloy thin film at zero field, prior to making the contact. In this particular template there is ~3 μm gap across the electrodes and the electrodes are 25 μm wide. (c) and (d) Schematic of moments going into the nanocontact (c) for electrodes with antiparallel aligned state (d) for electrodes with parallel aligned state.

(through the motion of the walls) domains that are favorably and unfavorably oriented with respect to applied field direction (and additionally by analyzing a weak optical contrast between adjacent domains since ICC is done using polarized light). The schematic in Fig. 5(e) shows that if such leads are joined together by a nanocontact, one would expect the magnetization to rotate along the nanocontact. The second schematic in Fig. 5(f) shows that even in cases where the opposite electrodes may be accidentally oriented in the same direction, a pseudo-90° domain wall may still form to adjust to the narrow, transverse boundary conditions in the nanocontact.

In case of thick Ni electrodes used in the present study (and also Co), we do not find the same well-defined domain structure as in Figs 5(a)–5(d). Instead, magnetization reversal occurs by the formation of hundreds of micron sized domains and these small domains appear to provide a high probability of an antiparallel aligned state across the nanocontact, collapsing into a parallel aligned state at high fields. As a visual aid, a movie showing evolution of domain structure in the electrodes as a function of applied field in Ni electrodes has been included as a supplementary material along with this paper, see Ref. 37 to access this movie from AIP's Electronic Physics Auxiliary Publication Service (EPAPS).

It is also interesting to note that conductance change can be observed in Figs. 4(a) and 4(c), where the initial conductance is $\frac{1}{2}G_o$ and $\frac{3}{2}G_o$, which would ordinarily refer to a parallel alignment of moments across the contact, as described by Imamura *et al.*[26] However the subtleties of the above described micromagnetic structure rapidly alter these states during the process of magnetization occurring at the electrodes and in the vicinity of the contact, and remains to be further explored. For example, a domain wall from the adjacent electrode may be swept towards the nanocontact during the process of magnetization. There also seems to be another micromagnetic structure that is possible in these contacts. Since the size is of atomic dimensions and the neck joining it to the adjacent electrodes has a very small volume, such a small volume of material would ordinarily be superparamagnetic *if it was isolated*. However, in case of a nanocontact, this small volume is joined together by bulk magnetic electrodes. The effective magnetic state at the constriction could still show superparamagnetic behavior albeit inside a reduced volume due to coupling with the bulk electrodes. Low temperature studies can be used to test this hypothesis in the future.

Garcia and Coey have performed experiments on *similar sized* atomic contacts as in this study.[1,4,5] They effectively show that for constrained and/or small electrodes of small size, magnetostatic distortions are negligible (of the order of 0.001 nm) and can be ruled out. In addition, our own direct experiments on the constrained geometry of small electrodes indicate the absence of magnetostatic distortions. We stopped the growth just prior to the formation of an atomic contact (or after an atomic contact breaks). When a magnetic field was applied across such an atomic scale gap between the electrodes, magnetostatic distortions, if present, would cause the formation of a contact and its breakup after the field is removed, and is not observed.

Another possibility is the field induced change in conductance by bringing new levels close to the Fermi level. Ordinarily the shift in energy levels due to applied magnetic field is miniscule. However, in these atomic contacts the quantum mechanical effects may well dominate to change the energy levels in an applied field. The observation of the above described fine structure in the inset of Fig. 4(a) is indicative and interesting in this regard. If realized, this would be an alternative *electronic* mechanism to MR requiring no domain walls.

Another possibility may be the physical breakup of an atomic contact and simultaneous formation of another atomic contact. Such an event would have to be highly synchronized and extremely rare in time, otherwise it would be immediately detected by a rapid drop in conductance below the threshold conductance of a single atom contact (we have used 10 000 scans/s to record the data). Hence this is an unlikely situation given also the fact that conductance coincides with applied field stimuli, the sample returns back to its initial conductance after the field is removed, and from sample to sample.

We note that the study of these atomic scale entities involves many subtleties to manifest the quantum expression of their behavior. Uncontrolled experiments can easily introduce artifacts, hiding the BMR effect. The present data is on quantum point contacts made of single atoms with conductance less than or equal to $2G_o$, and such contacts are undoubtedly ballistic and as we show the contacts never break, even when the contacts are tested at the threshold of quantized conductance. Conclusive elimination of magnetostriction related artifacts, which has been the most easily invoked primary alternative explanation to the electronic origin of BMR, is one step towards a better understanding of the BMR effect.

In the interest of scientific progress on BMR effect, it is also necessary to understand the origins of controversy surrounding the BMR effect. Recent work by Egelhoff *et al.*[38] has attributed BMR to magnetostriction and magnetostatic induced artifacts. The contacts in Ref. 38 are made between two bulk Ni wires, which are kept free and unconstrained to the substrate except for two points far from the actual contact. This *promotes* rather than hinders wire motion, thereby maximizing artifacts. For example, referring to Fig. 3 of Ref. 38, one finds that resistance changes from 1Ω or less to infinity. It is clear that the contact has broken in their measurements once the resistance value exceeds $\sim 13\,000\Omega$, whereas all previous results in BMR in the literature in favor of the effect never exceed this critical threshold. Looking at Fig. 7 of Ref. 38, there appears to be no correlation between the underlying domain structure and the magnetization process (two peaks each at positive and negative fields), which is again contrary to successful BMR experiments in the past by others.

Finally, there have also been reports of null effect in thin film samples, see for example, Refs. 39 and 40. From the above discussion on micromagnetic, note that absence of a multidomain structure in thin Ni films provides at least one plausible reason that could explain some of these null results, while at the same time explaining the recent observation of a large BMR effect across permalloy thin films.[8] Also, we have found the use of highly insulating substrate to be very important otherwise electrodeposition currents and leakage through the wafers occurs, and possibly destroying the BMR effect; we find no specific statement to this effect in reports of null results.

In conclusion, the present study on single atom Ni conductors irrefutably rules out any magnetostriction related artifacts in the measured BMR effect. Small distinctions in experiments may mean the difference between observing the BMR effect and disguising it with artifacts, thereby fueling the controversy. In addition, several explanations of null effects are reported in the literature.

Note added in proof. Observation of the BMR effect requires ballistic conductance whereas absence of BMR, at the minimum, requires proof of ballistic quantum behavior. Development of an appropriate micromagnetic structure is also indispensable. In Ref. 7 a multiplicity of parallel ballistic contacts was noted whose quantum nature was left to be determined. In this study, large BMR effect in artifact-free samples is from contacts that are unambiguously quantized and ballistic. It is important to note that an *infinite* number of nonballistic resistors may exhibit the same resistance as a quantum ballistic conductor. This is a simple, yet common mistake that must be avoided. We cite the recently failed observation of BMR by Mallett *et al.*[41] and Montero *et al.*[42] as examples of this misconception. Finally, in our recent experiments using the Co system, we have systematically measured large BMR effect and complete hysteresis loops, and these results will be reported shortly.[43] Our results show that for Co, the BMR decays very fast with contact size of quantum nature, and the effect becomes negligible for contacts larger than a few atoms.

This work was supported by NSF-DMR-03-05-242 and NSF-DMR-97-31-733, and this support is gratefully acknowledged. Microfabrication was done at the Cornell Nanofabrication Facility (a member of the National Nanofabrication Users Network), which is supported by the National Science Foundation Grant No. ECS-9731293 and Cornell University.

*Corresponding author. Email address: hchopra@eng.buffalo.edu

[1] N. García, M. Muñoz, and Y.-W. Zhao, Phys. Rev. Lett. **82**, 2923 (1999).
[2] N. García, M. Muñoz, G. G. Qian, H. Rohrer, I. G. Saveliev, and Y.-W. Zhao, Appl. Phys. Lett. **79**, 4550 (2001).
[3] N. García, M. Muñoz, V. V. Osipov, E. V. Ponizovskaya, G. G. Qian, I. G. Saveliev, and Y.-W. Zhao, J. Magn. Magn. Mater. **240**, 92 (2002).
[4] J. J. Versluijs, M. A. Bari, and J. M. D. Coey, Phys. Rev. Lett. **87**, 026601 (2001).
[5] O. Céspedes, E. Clifford, and J. M. D. Coey (unpublished).
[6] H. D. Chopra and S. Z. Hua, Phys. Rev. B **66**, 020403(R) (2002).
[7] S. Z. Hua and H. D. Chopra, Phys. Rev. B **67**, 060401(R) (2003).
[8] N. Garcia, H. Wang, H. Cheng, and N. D. Nikolic, IEEE Trans. Magn. **39**, 2776 (2003).
[9] For a recent review on the quantum properties of atomic sized conductors, see N. Agraït, A. L. Yeyati, and Jan M. van Ruitenbeek, Phys. Rep. **337**, 81 (2003).
[10] The total conductance is obtained by summing over all the open channels, and is given by the well-known Landauer-Büttiker equation, $G=(2e^2/h)\Sigma_{n=1}^{N}T_n$, Refs. 11 and 12. Here T_n is the transmission probability of the *n*th channel whose values range from 0 (closed) to 1 (fully open).
[11] R. Landauer, IBM J. Res. Dev. **1**, 223 (1957).
[12] M. Büttiker, Y. Imry, R. Landauer, and S. Pinhas, Phys. Rev. B **31**, 6207 (1985).
[13] T. Ono, Y. Ooka, H. Miyajima, and Y. Otani, Appl. Phys. Lett. **75**, 1622 (1999).
[14] M. Shimizu, E. Saitoh, H. Miyajima, and Y. Otani, J. Magn. Magn. Mater. **239**, 243 (2002).
[15] D. M. Gillingham, I. Linington, C. Müller, and J. A. C. Bland, J. Appl. Phys. **93**, 7388 (2003).

[16] D. M. Gillingham, C. Müller, and J. A. C. Bland, J. Phys.: Condens. Matter **15**, L291 (2003).

[17] Scheer *et al.* in Ref. 18 has shown that for a single atom contact, the number of channels is governed by the number of valence orbitals. For example, in a monovalent metal such as Au, the simple picture of one atom-one channel applies. In transition metals with incomplete *d* shell, a total of five channels contribute to the total conductance and the transmission probability T_n for each channel is generally less than 1. For instance, in a single atom Pt contact, the mean value of conductance has been shown to lie between $1G_o$ to $2.5G_o$ depending on strength of the coupling between the atoms, Ref. 19.

[18] E. Scheer, A. Agraït, J. C. Cuevas, A. L. Yeyati, B. Ludoph, A. Martín-Rodero, G. R. Bollinger, J. M. van Ruitenbeek, and C. Urbina, Nature (London) **394**, 154 (1998).

[19] S. K. Nielsen, Y. Noat, M. Brandbyge, R. H. M. Smit, K. Hansen, L. Y. Chen, A. I. Yanson, F. Besenbacher, and J. M. van Ruitenbeek, Phys. Rev. B **67**, 245411 (2003).

[20] S. Boussaad and N. J. Tao, Appl. Phys. Lett. **80**, 2398 (2002).

[21] *Atlas of Electrochemical Equilibria in Aqueous Solutions*, edited by M. Pourbaix, 1st ed. (Pergamon, Oxford, New York, 1966).

[22] M. R. Sullivan, D. A. Boehm, S. Z. Hua, and H. D. Chopra, (unpublished).

[23] E. W. Lee, Rep. Prog. Phys. **18**, 184 (1955).

[24] This of course is the upper limit since attaining saturation magnetostriction strain for Ni requires upwards of ~3000 Oe (based on our magnetization measurements), whereas only one-sixth of this value (500 Oe) was applied in the present study. In the presence of mechanical constraints preventing the Ni from changing its physical dimensions (such as the constraints imposed on thin film leads by the underlying substrate), the unrealized magnetostriction strain manifests itself as equivalent stress $\sigma^H = E\lambda^H$, where E is the Young's modulus (=20 GPa for Ni) and $\lambda^H(\leqslant\lambda_s)$ is the magnetostriction at field H.

[25] N. García, G. G. Qiang, and I. G. Saveliev, Appl. Phys. Lett. **80**, 1785 (2002).

[26] H. Imamura, N. Kobayash, S. Takahashi, and S. Maekawa, Phys. Rev. Lett. **84**, 1003 (2000).

[27] L. R. Tagirov, B. P. Vodopyanov, and K. B. Efetov, Phys. Rev. B **63**, 104428 (2001).

[28] L. R. Tagirov, B. P. Vodopyanov, and K. B. Efetov, Phys. Rev. B **65**, 214419 (2002).

[29] L. R. Tagirov, B. P. Vodopyanov, and B. M. Garipov, J. Magn. Magn. Mater. **258-259**, 61 (2003).

[30] L. R. Tagirov and K. B. Efetov, in *NATO Science Series II: Mathematics, Physics, and Chemistry*, edited by B. Aktas, L. R. Tagirov, and F. Mikailov (Kluwer Academic, New York, 2004), Vol. 143, p. 393.

[31] J. Velev and W. H. Butler, Phys. Rev. B **69**, 094425 (2004).

[32] P. Bruno, Phys. Rev. Lett. **83**, 2425 (1999).

[33] L. L. Savchenko, A. K. Zvezdin, A. F. Popkov, and K. F. Zvezdin, Fiz. Tverd. Tela (S.-Peterburg) (S.-Petersburg) **43**, 1449 (2001) [Phys. Solid State **43**, 1509 (2001)].

[34] V. A. Molyneux, V. V. Osipov, and E. V. Ponizovskaya, Phys. Rev. B **65**, 184425 (2002).

[35] J. M. D. Coey, L. Berger, and Y. Labaye, Phys. Rev. B **64**, 020407(R) (2001).

[36] H. D. Chopra *et al.*, Phys. Rev. B **61**, 15 312 (2000); H. D. Chopra, C. Ji, and V. V. Kokorin, *ibid.* **61**, R14 913 (2000); M. R. Sullivan and H. D. Chopra, *ibid.* **70**, 094427 (2004); H. D. Chopra, D. X. Yang, and P. J. Wilson, J. Appl. Phys. **87**, 5780 (2000);

[37] See EPAPS Document No. E-PRBMDO-70-046446 for accessing this movie, which shows the magnetization reversal in electrodes made of Ni. In the movie, the field is swept from negative to positive field, following saturation in the negative direction. The appearance of micron-sized domains in Ni and Co films appears at ~110 Oe, where the movies have been purposely slowed to better show the domain structure. A direct link to this document may be found in the online article's HTML reference section. The document may also be retrieved via the EPAPS homepage (http://www.aip.org/pubservs/epaps.html) or from ftp.aip.org in the directory /epaps/. See the EPAPS homepage for more information.

[38] W. F. Egelhoff, Jr., L. Gan, H. Ettedgui, Y. Kadmon, C. J. Powell, P. J. Chen, A. J. Shapiro, R. D. McMichael, J. J. Mallet, T. P. Moffat, M. D. Stile, and E. B. Svedberg, J. Appl. Phys. **95**, 7554 (2004).

[39] C. S. Yang, J. Thiltges, B. Doudin, and M. Johnson, J. Phys.: Condens. Matter **14**, L765 (2002).

[40] C. S. Yang, C. Zhang, J. Redepenning, and B. Doudin, Appl. Phys. Lett. **84**, 2865 (2004).

[41] J. J. Mallett, E. B. Svedberg, H. Ettedgui, T. P. Moffat, and W. F. Egelhoff, Jr., Phys. Rev. B **70**, 172406 (2004).

[42] M. I. Montero, R. K. Dumas, G. Liu, M. Viret, O. M. Stoll, W. A. A. Macedo, and I. K. Schuller, Phys. Rev. B **70**, 184418 (2004).

[43] M. R. Sullivan, S. Z. Hua, and H. D. Chopra, Phys. Rev. B (to be published).